

Multi-sensor core logging (MSCL) and X-ray computed tomography imaging of borehole core to aid 3D geological modelling of poorly exposed unconsolidated superficial sediments underlying complex industrial sites: An example from Sellafield nuclear site, UK

Nick T. Smith ^{a,b,*}, James Shreeve ^c, Oliver Kuras ^d

^a National Nuclear Laboratory, 5th Floor, Chadwick House, Birchwood Park, Warrington WA3 6AE, United Kingdom

^b Departments of Earth and Environmental Sciences and Mechanical, Aerospace and Civil Engineering, The University of Manchester, Oxford Roas, Manchester, M13 9PL, United Kingdom

^c Geotek Ltd, 4, Sopwith Way, Deventry, Northamptonshire, NN11 8PB, United Kingdom

^d British Geological Survey, Keyworth, Nottingham, NG12 5GG, United Kingdom

ARTICLE INFO

Article history:

Received 29 March 2019

Received in revised form 20 May 2020

Accepted 21 May 2020

Available online 23 May 2020

Keywords:

Multi-sensor core logging
X-ray computed tomography
Complex industrial sites
Superficial geology
Sellafield nuclear site

ABSTRACT

The 3D characterisation of geology underlying complex industrial sites such as nuclear plants is problematic due to the presence of the built infrastructure that restricts or in some cases completely prevents access for geologists to the subsurface environment. Outcrops are rare, geophysics surveys are often impossible (particularly at nuclear plants where activities such as vibroseis are frowned upon due to their effect on the infrastructure itself), and boreholes are often the only way to obtain subsurface data. Yet, with sedimentary deposits in particular, geotechnical logging undertaken to specific standards sometimes misses key information that could have been used to directly inform the creation of geological 3D models.

Multi-sensor core logging (MSCL) and X-ray computed tomography (XCT) undertaken on core obtained from a borehole within the Sellafield nuclear plant, is used to illustrate the potential for the techniques to contribute significantly to the creation of 3D subsurface geological models, particularly where access is restricted, such as within nuclear industry locations. Geophysical characteristics are recorded and used to reassess and enhance geotechnical descriptions, leading to the modification of existing unit boundaries or the creation of new ones. A new sedimentary log was created and this was used in a comparison with existing logs and nearby historic exposures, and as the basis for an illustration of industrial site to regional correlation.

© 2020 The Authors. Published by Elsevier B.V. This is an open access article under the CC BY-NC-ND license (<http://creativecommons.org/licenses/by-nc-nd/4.0/>).

1. Introduction

Undertaking geological investigation and characterisation at complex industrial sites such as nuclear power generation and reprocessing plants is typically beset with difficulty due to the availability of good quality, high resolution subsurface data. Suitable outcrop is either non-existent (depending on the geological objectives), limited in extent and coverage, or of such poor quality that it is not worth examining. Add to that restricted access, either due to site security issues, or the fact that the outcrop is often only revealed temporarily during the excavations for a new plant or building, and one is limited to intrusive or geophysical (low intrusive) methods to gain access to the geology. However, space to drill boreholes is extremely limited, whilst the aim of reducing costs means that nuclear decommissioning is often not afforded the luxury of fully cored boreholes with the retention of cores for later

examination also not possible due to environmental and other restrictions. Similarly, geophysical investigations are limited to down-hole geophysics or techniques such as microgravity surveys and magnetometry.

Information such as sedimentological and stratigraphic data, gathered from geotechnical borehole logs generated from techniques such as shell and auger or sonic drilling that are the mainstay of site investigation at all the UK's nuclear sites (and indeed, most industrial sites worldwide), is used to support conceptual model generation and to input into hydrogeological models (Turner, 2006; Zhu et al., 2012). Many 3D geological models are similar in that they are constructed to represent the sedimentary or stratigraphic system, such that 3D surfaces represent sedimentary or stratigraphic boundaries (Lemon and Jones, 2003; Smirnov et al., 2008; Tremblay et al., 2010; Zhu et al., 2012) although differences in techniques occur due to the use of different interpolation algorithms (Wellmann et al., 2010; Zhu et al., 2012).

Existing methods though, are fraught with limitations and shortcomings (Zhu et al., 2012), sometimes even resulting in geological

* Corresponding author at: National Nuclear Laboratory, United Kingdom
E-mail address: nick.t.smith@uknln.com (N.T. Smith).

models that differ from the actual geology, meaning that the computer model is either unreasonable or geologically invalid in some situations. This can be compounded when the geological description of the borehole log, typically undertaken according to geotechnical soil logging standards such as BS5930 (British Standards Institution, 2015) or Eurocode 7 (British Standards Institution, 2005), is less than satisfactory. For example, for those with interests in the lithostratigraphic development of an area are concerned, lithological boundaries defined under such standards are often not sufficient for stratigraphic correlation, particularly between industrial sites and regional interpretations. Indeed, where such ties have been attempted, they have typically been achieved using allostratigraphic principles (Rawson et al., 2002;

Räsänen et al., 2009) although these rely on correct identification of lithologies, unit boundaries and (for sedimentary geology), on the stratigraphic order of units, which site investigation boreholes often cannot supply. Hill, et al., noted: "Uncertainty is ubiquitous in natural hazards." (Hill et al., 2012, page 4), but in order to reduce uncertainty, we need to understand the geology in high resolution and its regional continuity in three dimensions, yet we cannot do this at present due to the complexity and nature of glacial soils/sediments within in the confines of standard logging practice.

Geophysical low intrusive techniques such as multi-sensor core logging ('MSCL' - Fresia et al., 2017), where sensors (e.g. non-destructive gamma-ray attenuation to measure bulk density, continuous P-wave

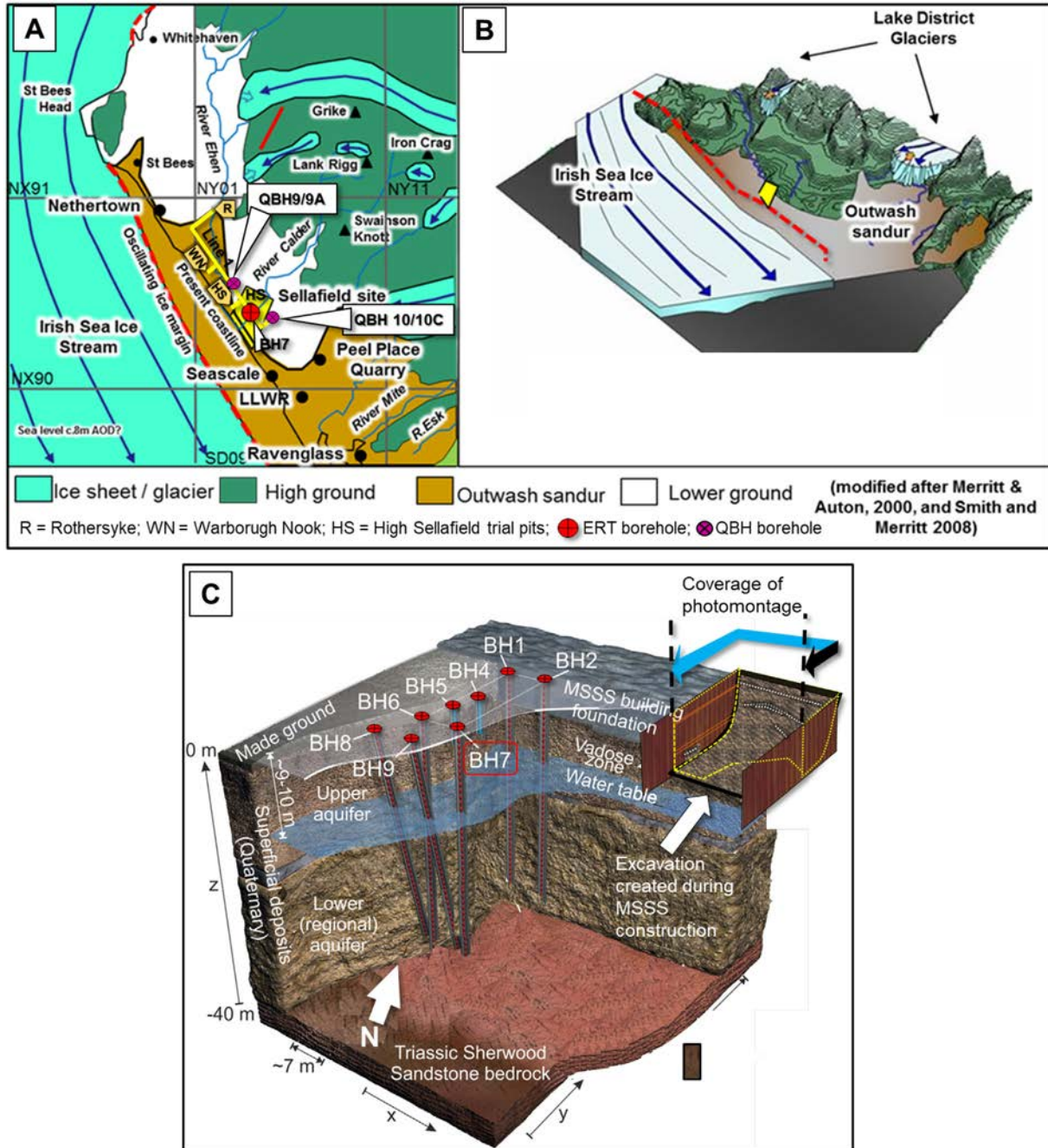


Fig. 1. (A) Regional location map, showing geography and geological setting; (B) 3D cartoon of glacial setting (Stage 8 of Merritt and Auton, 2000); (C) 3D detail of ERT boreholes (BH7 ringed in red), showing location of an excavation created during MSSS construction. ((A) and (B) modified from Merritt and Auton (2000) and Smith and Merritt (2008); (C) modified from Kuras et al. (2016)).

velocity, magnetic susceptibility) are used to scan borehole core at the drill site, may also address some of these issues and be particularly applicable to industrial sites where geological exposure is limited, improving geological understanding by increasing the resolution far beyond that achievable by traditional methods (e.g. studies by [Fellgett et al., 2019](#); [Gupta et al., 2019](#)). Indeed, as [Fresia, et al., \(2017\)](#) note, if many boreholes were logged using high-resolution, multiparameter measurements, then the 3D lithological understanding could also be improved. A combination of sedimentological logging (to a standard higher than the current logging standards), geotechnical information and geophysical data could vastly improve both site investigation and local, regional and national geological interpretations. This paper describes the application of such sensor and photonics technology to the logging and 3D geological modelling of Quaternary-aged superficial geology underlying Sellafeld nuclear site.

2. Study area and geological setting

Sellafeld nuclear site is located approx. 5 km south of Egremont on the narrow West Cumbrian coastal plain between the Irish Sea and foothills of the Lake District National Park ([Fig. 1](#)). Geologically the site lies partially on bedrock of the Mesozoic Sherwood Sandstone Group ([Jones and Ambrose, 1994](#); [Barnes et al., 1994](#); [Akhurst et al., 1997](#); [Kuras et al., 2016](#)) and partially on overlying Quaternary aged, glacially-derived sediments deposited during the main Devensian glaciation, and subsequent oscillations of the margin of the Irish Sea Ice Stream ([Busby and Merritt, 1999](#); [Merritt and Auton, 2000](#)). Nearby to the east, the foothills of the Lake District National Park are formed of volcanoclastic rocks of the Borrowdale Volcanic Group, and fine-grained, weakly metamorphosed, sedimentary rocks of the Skiddaw Group ([Akhurst et al., 1997](#)). These rocks form basement under the West Cumbria coastal plain.

The Quaternary history of West Cumbria has been relatively well established through studies associated with the aborted Nirex investigations and on-going studies associated with the Sellafeld and Low-level Waste Repository (LLWR) nuclear sites. It is generally agreed that the mountains of the Cumbrian Lake District the last major ice sheet glaciation took place during the Late Devensian Dimlington Stadial (28–13 ka). Tills containing granite and greywacke erratics derived from the Southern Uplands ([Trotter, 1929](#); [Trotter et al., 1937](#); [Eastwood et al., 1931](#); [Huddart, 1970, 1971a](#); [Huddart, 1971b](#); [Huddart, 1977](#), [Huddart, 1991](#); [Huddart, 1994](#); [Huddart and Tooley,](#)

[1972](#); [Huddart and Clarke, 1994](#); [Letzer, 1981](#)) occur towards the base of and higher in the sequence, indicating the movement of Scottish ice southwards into parts of the Cumbrian lowlands before the main Late Devensian glaciation, and the encroachment onto the coastal plain during the main Late Devensian glaciation ([Merritt and Auton, 2000](#)). Following this the Scottish Ice sheet underwent a number of glacial readvances ([Trotter, 1922, 1923, 1929](#); ; [Trotter and Hollingworth, 1932](#); [Trotter et al., 1937](#); [Huddart and Tooley, 1972](#); [Merritt and Auton, 2000](#)) depositing glaciofluvial and glaciomarine sediments which were overridden by ice, depositing thin veneers of diamictons ([Nirex, 1997](#); [Merritt and Auton, 2000](#)) including deformation tills ([Benn and Evans, 1998](#)).

The sediments deposited onshore in the West Cumbria area during the main Irish Sea Ice glaciation and the two identified readvance episodes typically comprise clay-rich diamictons (tills - [Benn and Evans, 1998](#)), separated by glacially-derived outwash sands and gravels, and lacustrine silts and laminated clays typical of an ice-margin sandur or ice-dammed lakes ([Merritt and Auton, 2000](#)), with the formal Quaternary lithostratigraphy defined by the latter.

Most recently, [Cross et al., 2018](#)) utilised the above understanding to support work investigating the susceptibility of the glacial deposits at Sellafeld to liquefaction under seismic loading conditions. However, geological interpretation of [Kuras et al. \(2016\)](#) of the vicinity of the borehole used in this study, represents the possibly first description of Sellafeld site geology in published literature, and utilised a simplified description of superficial geology based on correlating bulk lithologies. Description and subsequent correlation of units took into account depositional processes (i.e. lithofacies recognition, *sensu* [Rawson et al., 2002](#)), identification of erosion-bounding surfaces (*sensu* [Miall, 2006](#)) and an understanding of regional geology from published literature (although final correlation was based on recognition of lithological patterns ([Smith et al., 2008](#); [Kessler et al., 2009](#))). The defined lithostratigraphic outline is illustrated in [Fig. 2](#) which shows a schematic lithostratigraphic correlation between locations in the vicinity of Sellafeld site, comprising several natural or quarried exposures river cliff locations and a small number of boreholes (see [Fig. 1](#) for locations).

As shown, the geology comprises an alternating series of clay rich units (aquitards) interpreted as glacial tills, separated by outwash sands and gravels. For groundwater and subsurface contaminant modelling at Sellafeld site, the lateral continuity and extent, and the location of upper and lower boundaries of the aquitards are all of interest since better definition of these would allow higher resolution validation

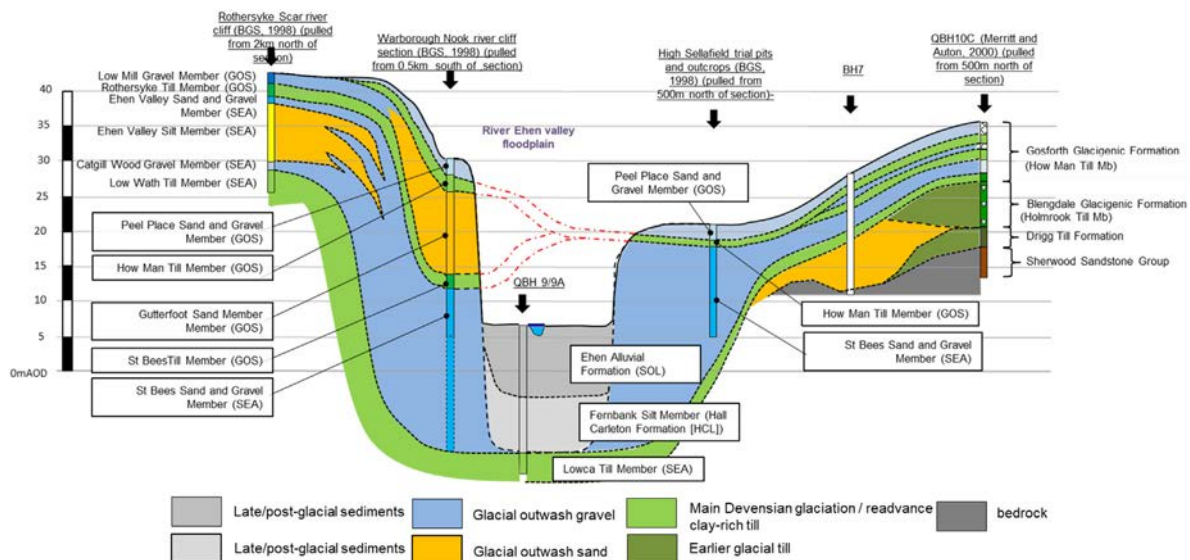


Fig. 2. Schematic cross section along line A ([Fig. 1](#)) – section and borehole information from ([Browne et al., 2000](#)).

of models and a reduction in uncertainty. In order to address these uncertainties, a detailed examination of core from borehole BH7 within Sellafield site was undertaken using low-intrusive geophysical core examination techniques including multi-sensor core logging and XCT deployed in an onsite mobile laboratory. The high-resolution information gathered from this is was converted into a full sedimentary graphic log which was then compared to a lithological log developed from the original BS5930/Eurocode 7 geotechnical log in order to assess changes to boundaries, lithological descriptions and resolution.

3. Using geotechnical logs as the basis for 3D geological modelling

3D geological models typically form the basis of hydrogeological models (Smith et al., 2008; Velasco et al., 2013). As shown in Fig. 3, borehole correlation panels can be created from borehole log descriptions. Often some rationalisation is required, for instance with units defined according to a simplification to bulk lithologies (e.g. CLAY, SAND, GRAVEL and SILT, sensu Rawson et al., 2002), which are obtained from geotechnical log descriptions, and ignoring all additional description. Unit boundaries are set by the original logged boundaries, providing correlatable units that start to resemble a glacial sequence of tills and outwash sands and gravels. However, the correlation shown in this panel and the resulting 3D model appear to bear only passing resemblance to the regional lithostratigraphic outline defined by Merritt and Auton (2000), such as is illustrated in exposures in beach cliffs on the West Cumbrian coast, which exemplifies the difficulties of correlating the Quaternary sequence within the Sellafield site to the lithostratigraphic outline outside.

The difficulties are compounded by the almost complete lack of exposure of any part of the Quaternary sequence within the site. Traditionally, site investigations within Sellafield nuclear site have been undertaken for construction or environmental monitoring purposes, and have involved the drilling of boreholes and the excavation of small trial pits. The latter provide some useful information, they invariably penetrate only the shallow sub-surface, often to no more than 5 m below ground level, and most of the exposure is of made ground (of which, as would be expected for such a complex industrial site, there is a not inconsiderable thickness). Excavations for construction of plants and buildings within the site have not usually afforded the opportunity to provide exposure suitable for geological study (as is often the case with industrial site investigation), leaving boreholes and trial pits as the predominant data source. At Sellafield, trial pits rarely penetrate below the not inconsiderable thickness of made ground that almost covers the whole site, so an excavation during construction of the Magnox Swarf Storage Silo (MSSS) at Sellafield site in the late 1970s afforded a temporary exposure of approximately 20 m thickness of Quaternary aged glacial sediments of which a number of sparsely annotated colour photographs provide useful geological information.

4. Multi-sensor core logging (MSCL) and X-ray computed tomography (XCT)

Multi-sensor core logging (MSCL) has been deployed for several decades and is particularly useful where downhole geophysics cannot be deployed (e.g. when drilling in deep water). C and M Schlumberger created the first geophysical log using electrical sensor arrays deployed down a borehole in 1929 (Goldberg, 1997), and by the 1960s techniques were being developed to log marine core using non-destructive gamma-ray attenuation to measure bulk density (Evans, 1970; Preiss, 1968). The processes were automated to a degree in the 1970s (Boyce, 1973) whilst the addition of further instruments obtaining data such as continuous P-wave velocity and magnetic susceptibility logs created a multi-sensor core logging (MSCL) system (Schultheis and McPhail, 1989; Schultheiss and Weaver, 1992). Natural gamma radiation (NGR) was first studied by Joly (1909), Faul (1954) and Adams and Gaspririni (1970) with

most procedures developed by the petroleum industry for borehole logging applications (Brannon and Osaba, 1956; Killeen, 1982; Flanagan et al., 1991), or for the purposes of deep borehole research (e.g. the system developed by Vasiliev et al., 2011), whilst the mining industry developed similar systems for prospecting uranium from airplanes (Lovberg et al., 1972; Gunn, 1978; Dickson et al., 1981; Gratsy et al., 1985). presented the first account of a device and procedures to measure NGR routinely on long sediment cores and perform spectral data analyses and NGR is now a regular feature of MSCL. Aside from lithological characterisation, additional applications have been developed, including the characterisation of mineralisation and hydrothermal alteration (Fresia et al., 2017), leading to further developments including visible and near infrared spectroscopy and portable X-ray fluorescence (pXRF) (Herrmann et al., 2001; Gazley et al., 2014; Yang et al., 2011; Durance et al., 2014; Fisher et al., 2014; Gazley and Fisher, 2014; Le Vaillant et al., 2014). More recently, as a result of improvements in technology, X-ray computed tomography (XCT), originally developed as a medical imaging technique (Hounsfield, 1972, 1973), has been utilised for the 3D

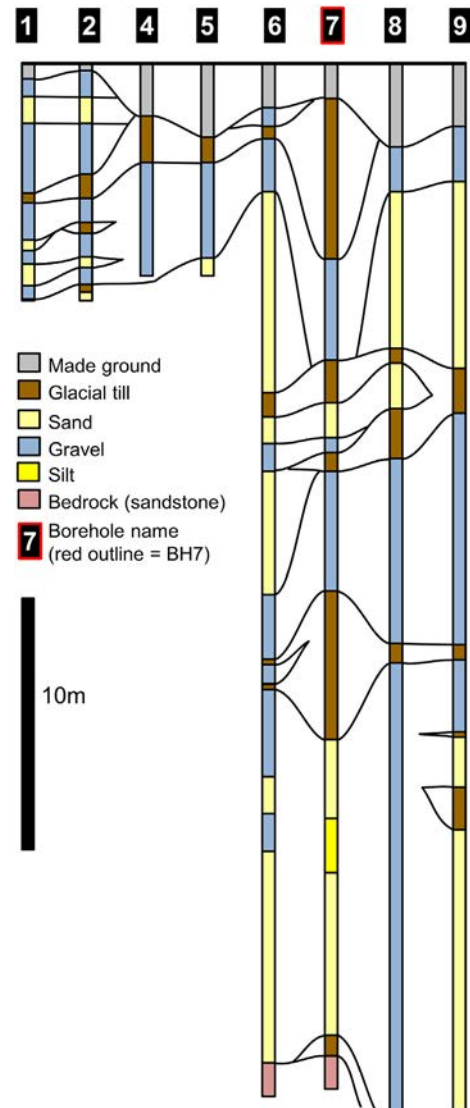


Fig. 3. Schematic borehole correlation panel for ERT boreholes created using geotechnical log (AGS) (units defined from bulk lithologies - grey = made ground; brown = clay; blue = gravel/sand & gravel; ivory = sand; yellow = silt) (horizontal: to scale).

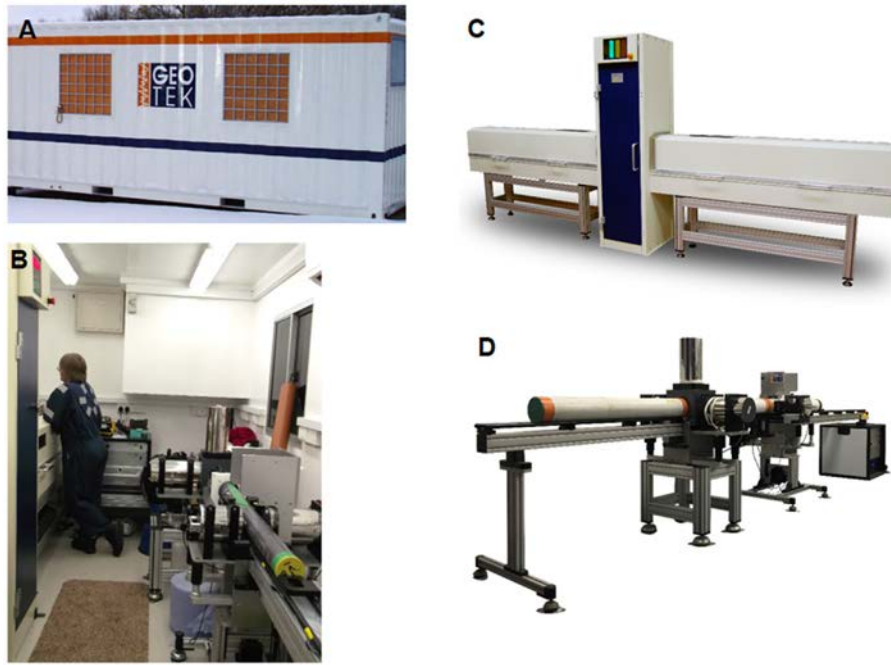


Fig. 4. MSCL-XCT and MSCL-S instrumentation and field deployment set up: (A) and (B) containerised mobile laboratory; (C) XCT (X-ray Radiographs and X-ray CT); (D) MSCL-S (natural gamma, gamma density, electrical resistivity, magnetic susceptibility, P-wave velocity).

imaging and analysis of the internal structure of geological materials such as rocks, soils and fossils (Petrovic et al., 1982; Haubitz et al., 1988; Cnudde and Boone, 2013; Ketcham and Carlson, 2001; Mees et al., 2003). The technique has seen further application with examination of borehole core in order to understand 3D textural relationships (e.g. in ore geoscience) (Becker et al., 2016; Jardine et al., 2018)

MSCL-XCT data also provide lithological information, whilst visual examination of XCT radiographs provides information about sedimentary and deformation structures. Whilst some of these features may be present to the naked eye, the disturbed nature of the outside of the core resulting from its extraction from the borehole and the liner means it is simply not possible to obtain information to the resolution that MSCL-S and XCT will allow.

5. Materials and methods

5.1. Materials

The study utilised core obtained from one of six deep boreholes drilled as part of a project designed to monitor contaminant plumes in groundwater beneath the Magnox Swarf Storage Silo (MSSS) at Sellafield nuclear sites in the UK. A full description of the boreholes drilled is provided in Kuras et al. (2016). This study is based on core obtained from borehole BH7 which was drilled between August and October 2012, using rota-sonic drilling to penetrate a thin veneer of artificial made-ground and just under 40 m of glacially-derived superficial material, before bottoming out in Triassic-aged bedrock of the Wilmslow Sandstone Formation (Sherwood Sandstone Group). Core was examined and logged behind a barrier system (as per safety procedures within that part of Sellafield site), before being transferred to a mobile MSCL laboratory stationed close to the borehole within the barrier system.

The study utilised a multi-sensor core logging 'Geotek MSCL-S' instrument and cabinet-based X-ray Computed Tomography (XCT) instrument combination installed in a mobile laboratory (Fig. 4A and B), operated by Geotek personnel.

5.2. X-ray computed tomography (XCT)

The cabinet-based XCT instrument (Fig. 4 C) uses 2D transmission of X-rays through the sample (in this case a borehole core) at multiple angles to create a 3D volume. This is then 'sliced' vertically to produce 'core slices'. These radiographs provide images from the core as if it was sliced vertically and one was able to view the cut face of the slice. CT data was acquired over geologically interesting areas of the core, with radiographs at multiple angles acquired from all samples.

All X-ray images are positive (i.e. dark objects are denser), which is the inverse of medical X-rays. Image resolution of the initial 2D radiographs is $\sim 100 \mu\text{m}$. Image resolution of the CT from the combined 3D volume data is $\sim 200 \mu\text{m}$.

5.3. MSCL-S

MSCL-S (Fig. 4 D) is a non-destructive petrophysical and geochemical core logging platform that can acquire measurements without direct contact with the sediment core. This means core can be examined through a core liner. This is particularly useful for nuclear sites where regulatory and space restrictions may mean that extraction of the core itself from the liner is impossible. The MSCL-S instrumentation gathers the following data:

- Natural gamma - represented here by a line graph coloured pink underneath the line
- Normalised gamma: represented by a dashed pink line
- Resistivity: represented by a colour coded filled graph, with dark blue for 0.1 Ohm m red for 100 Ohm m.
- Density: red line graph (1-3 g/cc)
- Fracture porosity: (0-1) blue line graph

6. Lithological characteristics from BH7 MSCL-S and XCT data

A comparison of MSCL-S and XCT data with borehole descriptions and published information, including literature on the regional

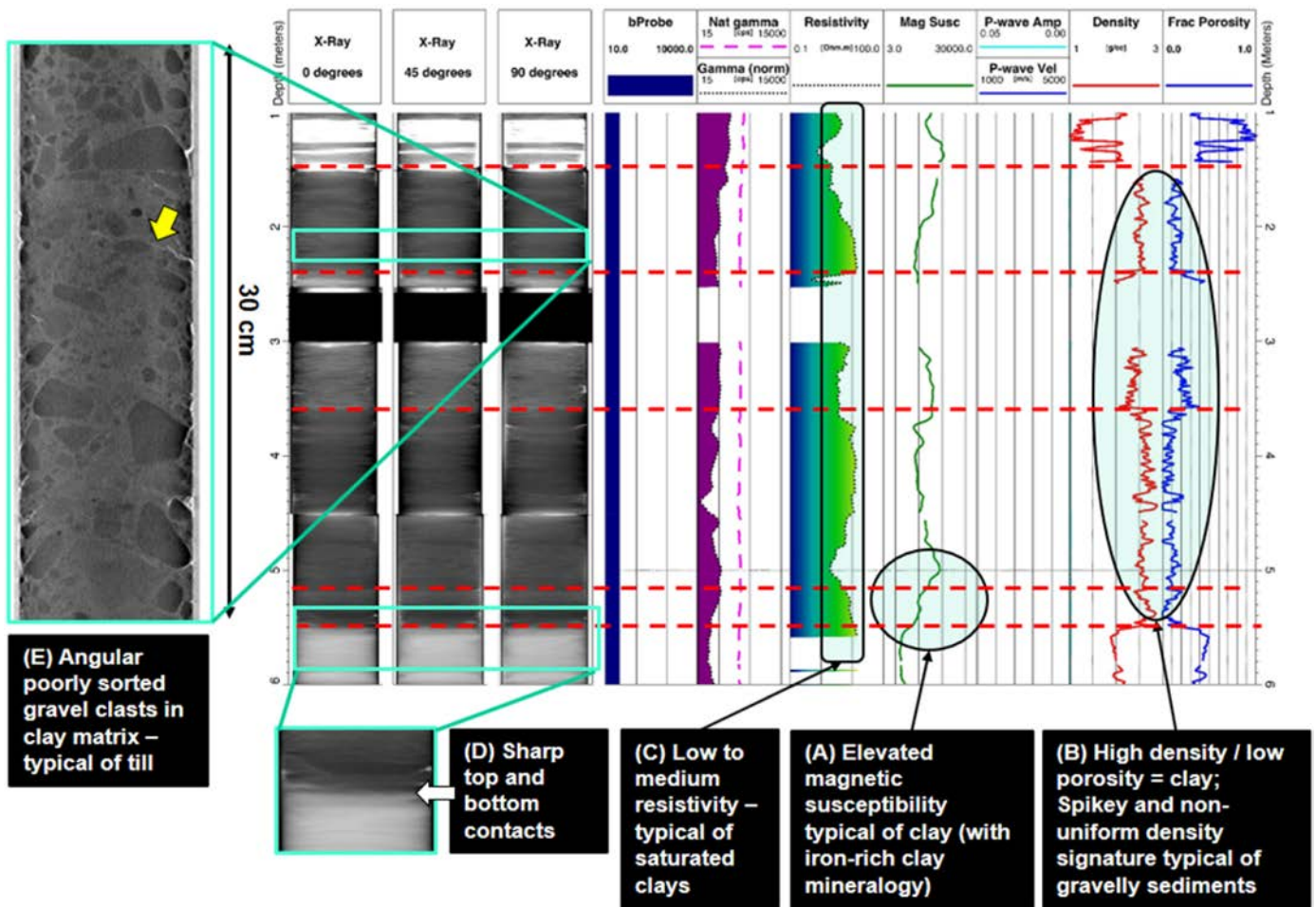


Fig. 5. MSCL and X-ray characteristics of clay-rich diamicton (till) lithologies within BH7 (1 m–6 m BGL – see Fig. 8 for vertical location).

Quaternary geology, enables the development of an understanding of geophysical characteristics which are described here.

6.1. MSCL and X-ray characteristics of clay-rich diamicton (till) lithologies

The lithological characteristics of glacial till exposed in West Cumbrian coastal outcrop have been well described by Merritt and Auton (2000), Akhurst et al. (1997) and authors of commercial reports (e.g. Smith and Cooper, 2004). Key characteristics identified from field exposures and boreholes include the presence of clay either as the main lithology or as a matrix supporting other lithologies including gravel and silt; poorly-sorted angular-grained gravels and sharp basal and top contacts typical of erosive sequences (Merritt and Auton, 2000). In deformation tills, the latter also note the presence of penetrative glacitectorite features within sediments directly underlying till units, including a high degree of compaction and shear fractures permeating up to 1 m below the low boundary of a till. Smith (2009) identified a penetrative glacitectorite beneath an extensive brown/grey till unit within the excavation for a disposal vault within the Low Level Waste Repository site, which includes slivers and lenses of clay present within 30 cm of the lower boundary of a deformation till. Tills typically contain clasts representative of geology the glacier has travelled over. For example, clasts of Lake District rocks from units such as the Borrowdale Volcanic Group (BVG) are found in tills derived from Lake District Glaciers (e.g. the Holmrook Till Member), whilst those deposited by the Scottish Ice Sheet are characterised by the presence of Scottish rocks such as

granite fragments from the Southern Uplands (Akhurst et al., 1997; Merritt and Auton, 2000).

Examination of the geophysical data compared with the core descriptions shows that clay-rich, stony diamicton (till) lithologies present within BH7 possess an array of MSCL characteristics that reflect their composition and depositional environment, leading to the identification of three lithofacies. Key characteristics include: (a) a low-to-medium natural gamma count, corresponding to the findings of (Cripps and McCann, 2000); (b) a high magnetic susceptibility (Robinson, 1993); (c) low-to medium resistivity; and (d) a relatively high density (with a corresponding low porosity), but with a spikey and variable density signature. The X-ray radiographs provide evidence of pure and laminated clays but gravel-rich clays predominate, with clasts ranging in size from a few millimetres to several centimetres, and in shape from angular to rounded, with most clasts being angular.

The high magnetic susceptibility (Fig. 5(A)) may be an indication of the composition of gravel clasts if they are present, but is much more likely to indicate clay matrix which has magnetic elements such as iron present within the clay mineralogy (Robinson, 1993). The magnetic susceptibility profile changes: abruptly wherever there are abrupt changes in density, indicating changes in material composition, such as variations in clay content from a till to an outwash unit, or gradually, for instance, when gravel clast size changes through a unit, or in the presence of sedimentary structures (Robinson, 1993).

The spikey and variable density signature itself (Fig. 5(B)) results from the gamma beam passing through heterogeneous gravels.

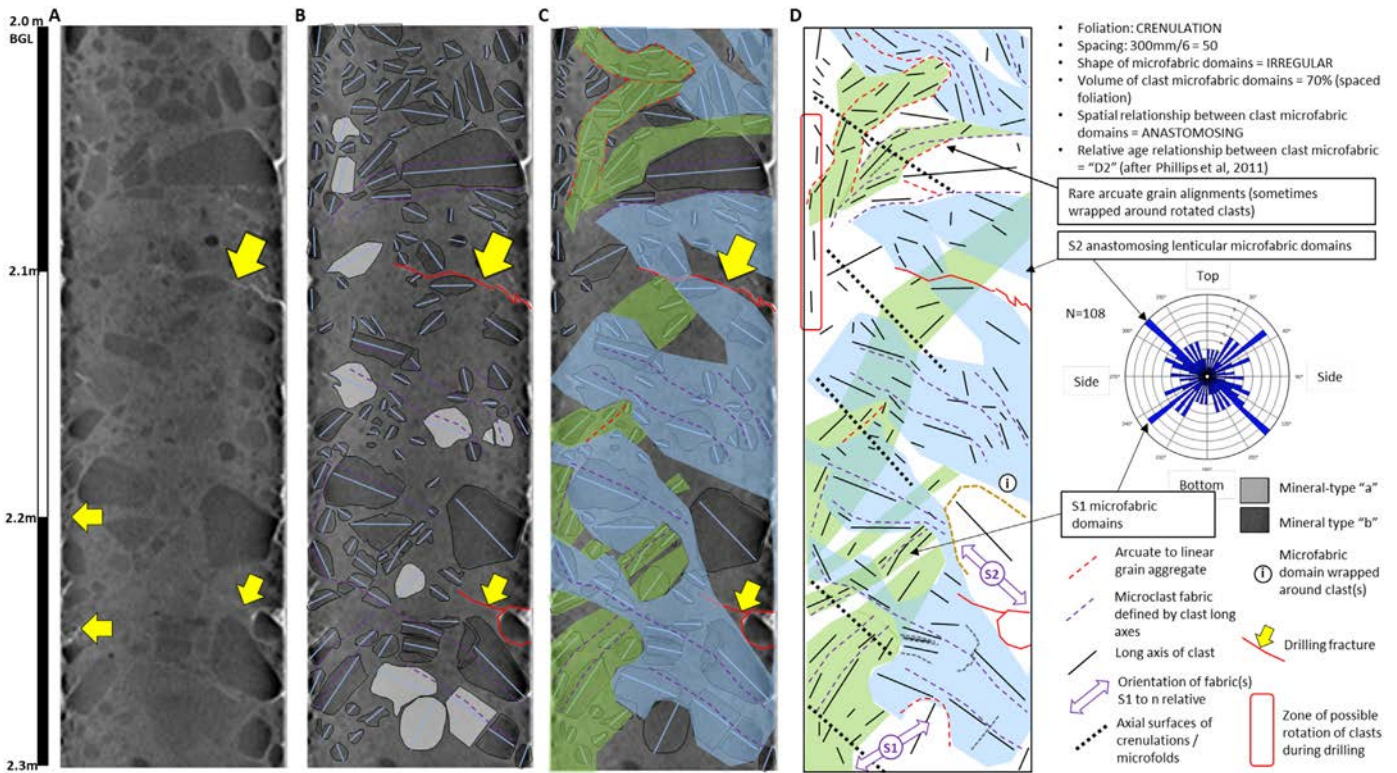


Fig. 6. (A) X-ray computed tomography (XCT) image of clay-rich diamicton core from 2 to 2.3 m BGL in BH7 (see Fig. 8 for vertical location), Sellafield nuclear site – note clasts and clay rich matrix (as indicated in MSCL data); (B) clast long-axis orientations plotted. Grey shading indicates clasts of different lithology to majority of clasts; (C) microfabric domains plotted (green = S1 domain; light blue = S2 domain); (D) interpretation with XCT image removed – note microclast fabric lines (purple dashes), arcuate to linear grain aggregate, sometimes wrapped around larger clasts. S1 fabric is overprinted by S2 fabric. NB large yellow arrows indicate cracks and fractures that probably formed during drilling, and a zone of rotated clasts with long axes rotated so they are vertically aligned, which may also have formed during drilling.

Resistivity measurements are usually high for gravelly sediments with little clay present, and low for clay-rich sediments (the high amount of water present in the pore structure increasing electrical conductivity) (Gunn and Best, 1998), and the evidence supports this with a low to medium resistivity profile, relative to the resistivity profile for gravel (Fig. 5(C)).

However, it is the X-ray radiographs that have a real visual impact. For example, in Fig. 5(D) the shapes of gravel clasts are obvious, enabling one to define both angular and rounded clasts, as is the poorly sorted nature of the sediment, both of which are typical of a till diamicton (Benn and Evans, 1998). Angular clasts appear to dominate however, also reflecting the nature of the highly visible sharp basal and top contacts typical of erosive sequences, are visible within the X-ray radiograph (Fig. 5(E)). These correspond to abrupt changes in magnetic susceptibility, density and resistivity, and almost certainly also represent abrupt changes in sediment type and material composition (e.g. clay or gravel mineralogy). It is also important to note that the greyscale values of the X-ray images reflect changes in density, with dark colours representing high density.

There is no P-wave profile, which is assumed to be due to a combination of attenuation of the signal resulting from cracks within the sediments (e.g. yellow arrow in Fig. 5), the orientation of which suggests formation during drilling, and the high frequency of the signal, although the casing may also attenuate the signal on its way to the core. Gravelly lithologies can also cause some interference when there are many present within the samples (Schultheis and McPhail, 1989).

The X-ray radiographs are also very useful for imaging sedimentary structures such as lamination and cross-lamination, which provide extra information for correlation purposes, and even information useful in the assessment of sedimentary architecture (actually part of this study but not addressed in this paper).

6.1.1. Deformation within subglacial tills

Over the years of study there has been much discussion of whether or not the clay-rich sequences penetrated by boreholes within and in the vicinity of the Sellafield nuclear site are "tills" per se (i.e. deposited sub or supra-glacially) or simply clays deposited in ice-dammed, glacial lakes located in an ice-marginal trough or sandur.

The identification of angular clasts within a clay rich matrix on XCT images (Fig. 5(E)), provide additional evidence to the observations recorded on the geotechnical logs, and the interpretation of MSCL data, that the lithology at 2mBGL in BH7 (for example) is almost certainly a diamicton, or till. However, although several types of till have been noted in the west Cumbria region, including subglacial deformation tills, melt-out tills and lodgement tills (Merritt and Auton, 2000), there could be an argument that some of these are lacustrine, and that the gravel has arrived via glacial outwash.

Subglacial diamictons have often undergone several phases of deformation through either several multiple deformation events representing separate pulses of ice advance and retreat, or a single progressive event relating to a single phase of ice advance (Phillips et al., 2011). The latter authors developed a methodology for the recognition, analysis and interpretation of the interrelationships between the various microstructures developed within diamictons, based on the application of structural geology techniques and nomenclature undertaken by a number of authors (Phillips and Auton, 2000; van der Wateren et al., 2000; Phillips et al., 2007; Denis et al., 2010). Here, the same methodology is applied to XCT images of glacial diamicton within the BH7 core, utilising the XCT image as if it were a thin section. The whole XCT image in Fig. 6 is of comparable size to the thin sections described by Phillips, et al., (2011), although the resolution is poorer, it does provide the basis for interpretation of a plane within the core itself, and whilst the actual orientation of the image relative to the location of the

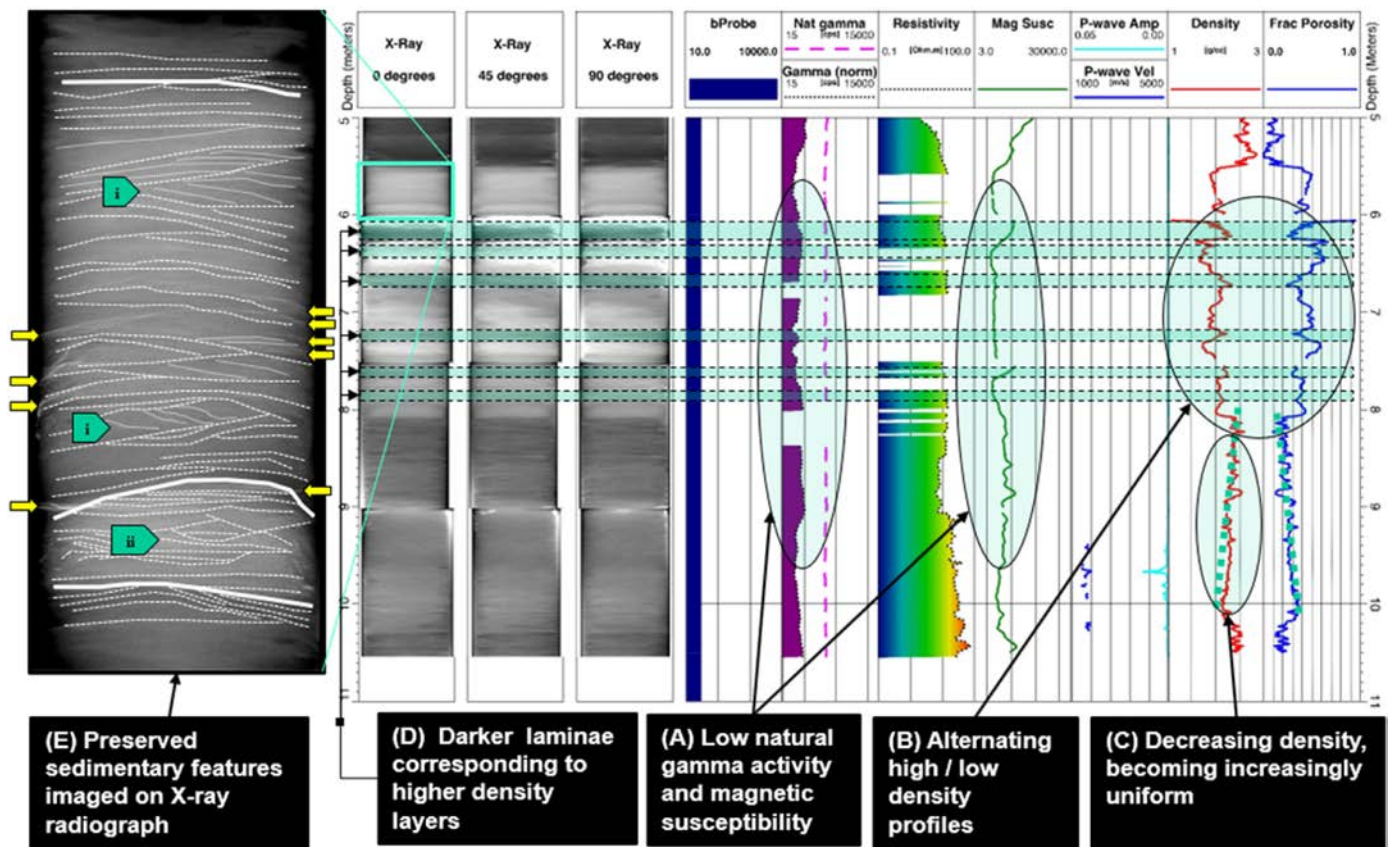


Fig. 7. MSCL and XCT features of glacial outwash lithologies. E(i) = planar cross bedding; E(ii) = trough cross (yellow arrows indicate fractures produced during coring) (see Fig. 8 for vertical location).

borehole itself is lost, a number of observations can be made that show unequivocally that the deposit is a deformation till.

In Fig. 6(B), long axes of clasts are plotted onto the image, as per Phillips, et al., (2011). Clasts of different colouration are an indication of different minerals, highlighting potentially different provenances. Yellow arrows show fractures that probably developed during drilling as suggested by their orientation.

The relative orientations of 108 clast axes have been plotted on a rose diagram illustrating the presence of two microfabric domains. Clast microfabrics are indicated by purple dashed lines in Fig. 6(C), whilst rare arcuate to linear grain aggregates (some of which wrap around larger clasts) are indicated by red dashed lines. Microfabric domains are shaded in light green and light blue. Examination of the two shows that the blue shaded domain (S2 fabric) overprints the green (S1) fabric, suggesting the deformation event that caused structures in S2 occurred later than those in S1. Fig. 6(D) removes the underlying XCT image, enabling better examination of these features. It is also possible to identify small crenulation folds within the S1 fabric, and axial surfaces (represented by black dotted lines) are shown to be parallel to the S2 fabric, suggesting the folds formed during formation of that fabric. Orientations of fabrics and folds show that the relative age relationship between clast microfabrics is “D2”. Following the approach of Phillips, et al., (2011), it is also possible to note that the S2 microfabric is spaced, irregular and anastomosing, with an irregular shape and a spacing of 50, whilst the S1 fabric is spaced with a smooth or continuous foliation (Phillips et al., 2011).

The ratio of clast to matrix indicates a matrix-supported till, which would have enabled a relatively high fabric intensity due to the open packing of clasts allowing them to rotate more easily. As the till progressively dewatered, clast rotation was gradually impeded, leading to a stiffening of the till. However, although dewatering occurred, water

saturation was maintained by the impermeable nature of the clay-rich matrix (as indicated by the MSCL data described above) which inhibited intergranular pore water flow (van der Meer, 1993, 1997), meaning the stiffening effect actually took some time to occur, resulting in a well-developed S1 and S2 fabrics, emplaced during variations in ice movement.

Although only one XCT image is shown here, three images with orientations at 45° to each other, were actually available, offering potential for a full 3D reconstruction of the original dip and strike of fabrics using (for example) lower hemisphere stereographic projection, as proposed by Phillips, et al., (2011).

Thus, even from a single orientation XCT image there can be no doubt about the interpretation of the unit as a subglacial deformation till (sensu Benn and Evans, 1998), but as the above shows, further interpretation is possible, leading to a greater understanding of depositional, structural and stratigraphic evolution. This is important, because subsequent correlation with interpretations from other boreholes can contribute greatly to 3D geological modelling of similar lithologies or lithofacies.

6.2. MSCL and X-ray characteristics of glacial outwash lithologies

MSCL-S and XCT-radiograph features that are characteristic of glacial outwash lithologies are shown in Fig. 7. Within MSCL data, borehole core with a very low natural gamma profile (Fig. 7A) indicates sediments with a lower clay content (Cripps and McCann, 2000), a typical feature of outwash sediments where the clay has been washed out (Benn and Evans, 1998). Quartz (a key component of silty and sandy outwash lithologies) is diamagnetic, which means its presence reduces the magnetic field strength sensed by the magnetic susceptibility sensor, so a low magnetic susceptibility is a good indication that sandy

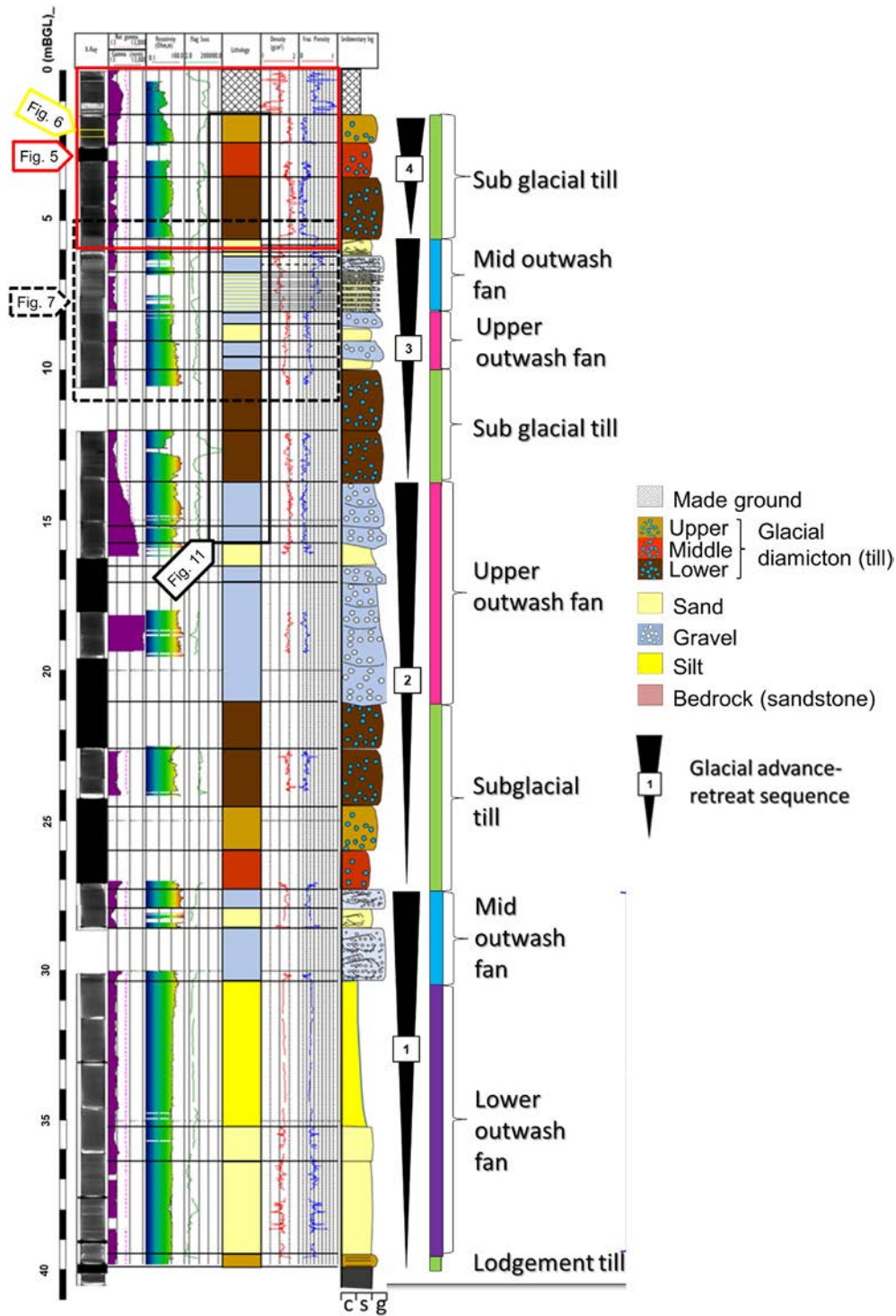


Fig. 8. Fully revised graphic sedimentary log for BH7 (note rectangles showing locations for Fig. 5 [red], Fig. 6 [yellow], Fig. 7 [black dashed] and Fig. 11 [black solid]). Note how this aids the transition from the first correlation (Fig. 3) to the revised version in Fig. 10, and how this aids interpretation of geological history as per Fig. 9.

lithologies are present whilst clay content is poor (in contrast to till which is typically clay-rich).

Silts, sands and gravels typically produce a low-density profile, so alternating sequences of low and high density (Fig. 7B) representing interbedded less-dense and dense laminae, with the latter probably due to an increase in clay/silt within pore space. It is likely these represent higher-energy, sand or gravel units (less dense), interbedded with lower energy, silt or clay units. An overall downward reduction in

gamma, density (Fig. 7A) and magnetic susceptibility, results from a decrease in grain size from top to bottom, indicating a coarsening-upwards sequence and vice versa.

The XCT-radiograph captures sedimentary structures such as planar and trough cross bedding (Fig. 7E (i) and (ii) respectively), which when viewed in 3D can provide an even better assessment of the 3D sedimentary architecture. The high-resolution nature of the MSCL and XCT image data here enables far more precise determination of contacts

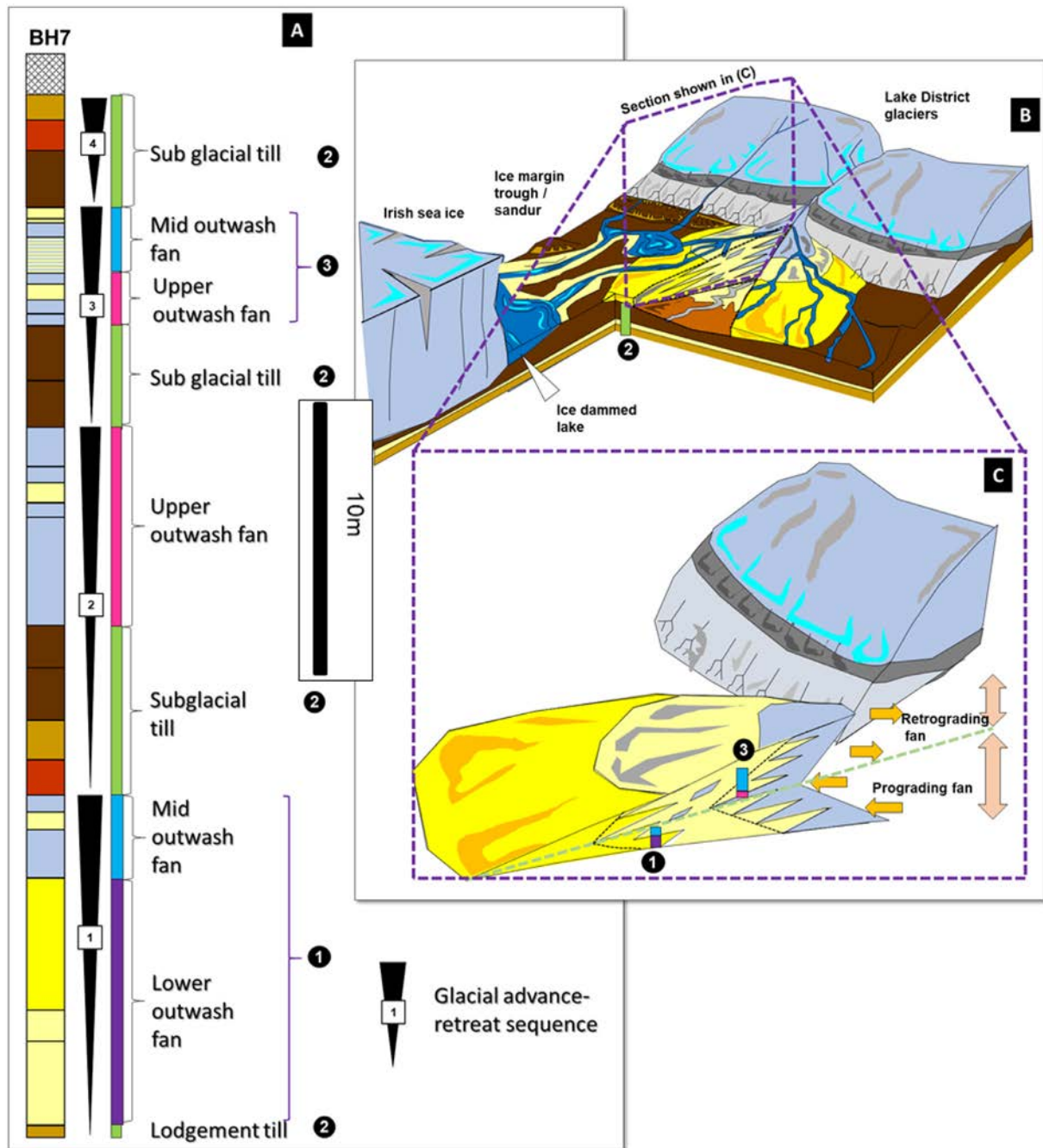


Fig. 9. (A) Simplified log for BH7 showing depositional cycles represented by glacial advance/retreat sequences, and interpretations of the main components of each sequence; (B) and (C) 3D interpretation showing how the interpreted log can provide information on the 3D depositional environment (here showing how outwash sequences were likely to have been deposited in prograding and retrograding fans within an ice-marginal trough or sandur).

than the traditional geotechnical log allows, leading to a firm identification of thinner units not possible through examination of core from glacial sediments with the naked eye.

7. Graphic sedimentary log

Based on the geophysical characteristics described above it is possible to identify similar features within the whole MSCL-S and -XCT dataset for the full extent of the cored sections of BH7. This information has been used to update the existing geotechnical log descriptions, re-define boundaries between lithological units, and identify new lithological units (and thus identify new boundaries between units). The new lithological descriptions are much more descriptive than those required

under the geotechnical site investigation standards, being more like those that form the basis of sedimentary graphic logs. In fact, it is the latter that can (i) help better identify the laterally extensive and (potentially) laterally continuous interfaces that form sequence and other boundaries, which often mark the tops or bases of the permeable or impermeable layers that are so critical to groundwater movement (Lemon and Jones, 2003); and, (ii) enable more geologically valid correlation of lithostratigraphic units. Correlation of these units and surfaces from borehole to borehole enables the creation of 3D/4D geological models that are much more valid in terms of hydrogeological modelling (Lemon and Jones, 2003).

A new graphic log for BH7 has been developed (Fig. 8) utilising the data and interpretation developed during this study. A number of

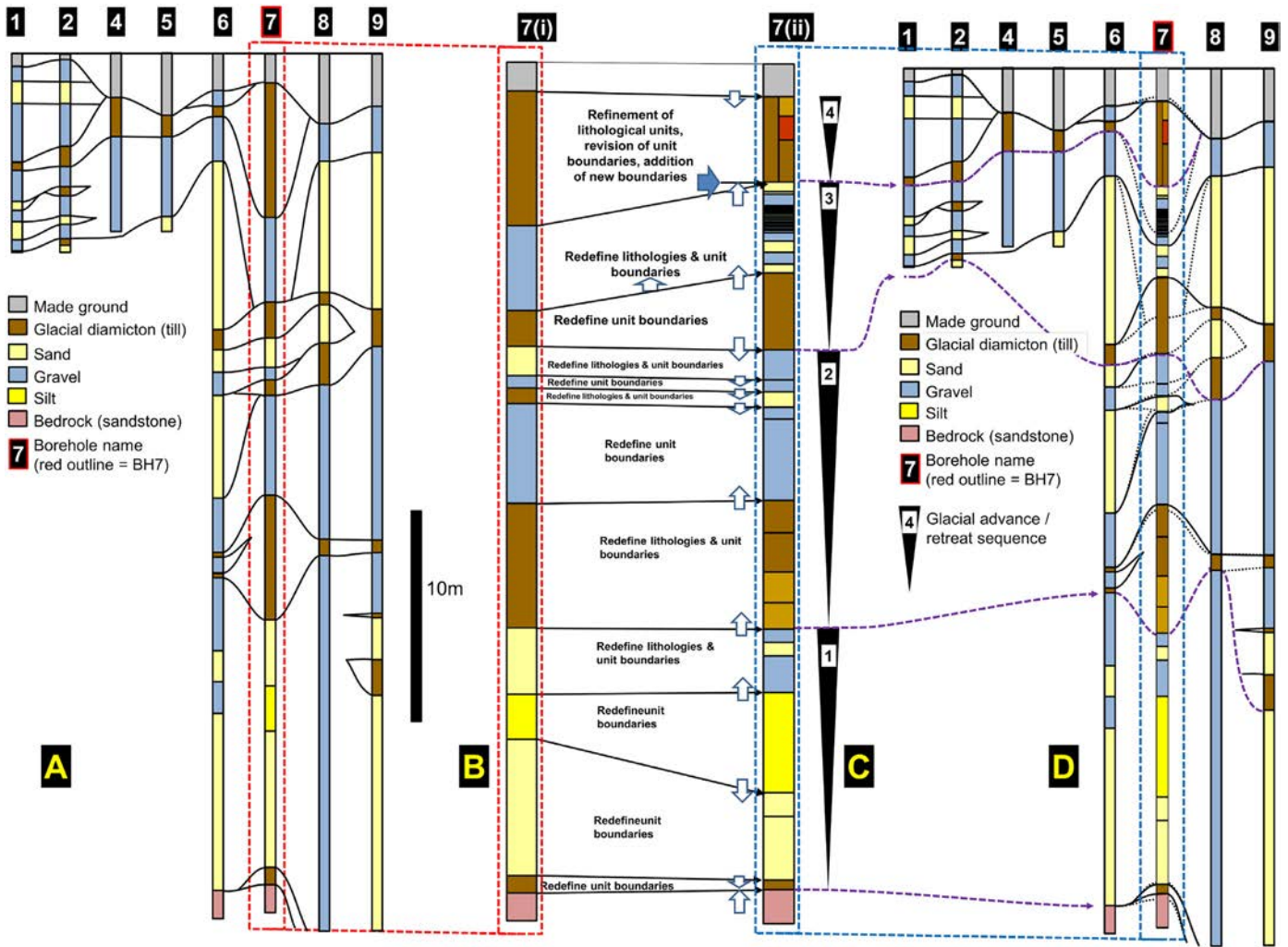


Fig. 10. (A) Original borehole correlation panel based on identification of bulk lithologies; (B) original lithology log for BH 7, based on bulk lithology descriptions from BS5930/Eurocode7 geotechnical log description; (C) modified lithology log for BH7 created using updated geotechnical log descriptions obtained from MSCL & XCT descriptions, showing better defined units and bounding surfaces; (D) modified log reinserted into borehole correlation panel (dashed lines = previous unit-bounding surfaces – note how unit boundaries have changed compared to (A)). Note mapping of glacial advance / retreat cycles (represented by Sequences 1 to 4) onto borehole panel erosion surface unit boundaries.

lithologies can be identified which together form the framework of a sequence of repeating cycles (four in total), each one of which is characterised by a lower sequence of clay-rich diamictons (see also Fig. 3, Fig. 9A, Fig. 10 and Fig. 11) overlain unconformably by an upper sequence of dominantly glacio-fluvial lithologies comprising repeated fining-upwards cycles of coarse-grained (up to boulder-sized) gravels overlain by sands and finer silts (Fig. 9A). Glacio-fluvial sequences represent outwash deposition during glacial retreat or deglaciation (Smith, 1932), with much coarser material representing proximal (upper) parts of an alluvial fan system depositing material over a sandur at the head of a glacier, whilst finer materials represent more distal (lower) parts of the fan system (Miall, 2006; Thomas et al., 1985; Thomas and Chiverrell, 2007).

The clay-rich, coarse-grained diamictons of the lower parts of each fining-upwards cycle contain coarse, angular clasts and evidence of structural deformation and are typical of subglacial deformation tills (sensu Benn and Evans, 1998). Based on geophysical information it was also possible to subdivide some of the till units into lower, middle and upper units comparable to those identified by authors such as (Larsen and Piotrowski, 2003). These probably formed in comparable ways to models of (Boulton and Jones, 1979; Boulton and Hindmarsh, 1987; Hickock and Dreimanis, 1992; Benn, 1995; van der Wateren, 1995; Larsen and Piotrowski, 2003).

Although the log in Fig. 8 represents a single vertical section through the glacial succession, the fact that each lithofacies is likely to vary laterally in lithofacies means that it can provide a useful guide as to the 3D and even 4D lithostratigraphic evolution of that particular area within Sellafield site, thus providing further useful information for incorporation into 3D geological and hydrogeological models at site. The four cyclic depositional sequences are clear in Fig. 9(A): Sequence 1 comprises a thin lodgement till at its base, resting directly on Triassic-aged sandstone bedrock of the Sherwood Sandstone Group (Smith and Cooper, 2004). This unit is reminiscent of the Lowca Till Member a lodgement till identified at the base of the cliffs at St Bees (Browne et al., 2000; Merritt and Auton, 2000). Over this lies a coarsening upwards sequence of silts, sands and gravels interpreted as lower outwash fan deposits overlain by mid outwash fan deposits sensu Thomas and Chiverrell (2007) and illustrated by (1) in Fig. 9(C). Sequence 2 comprises a subglacial till, which has been divided into three sub-lithofacies sensu Larsen and Piotrowski (2003) and is illustrated by Fig. 9 (2). This is overlain by coarse grained gravels and sands interpreted here as upper outwash fan deposits. Similarly, Sequence 3 comprises sub-glacial till overlain by medium to coarse-grained sands and gravels. The latter probably represent upper outwash fan deposits at the base and mid outwash fan deposits towards the top (i.e. the sequence is reversed

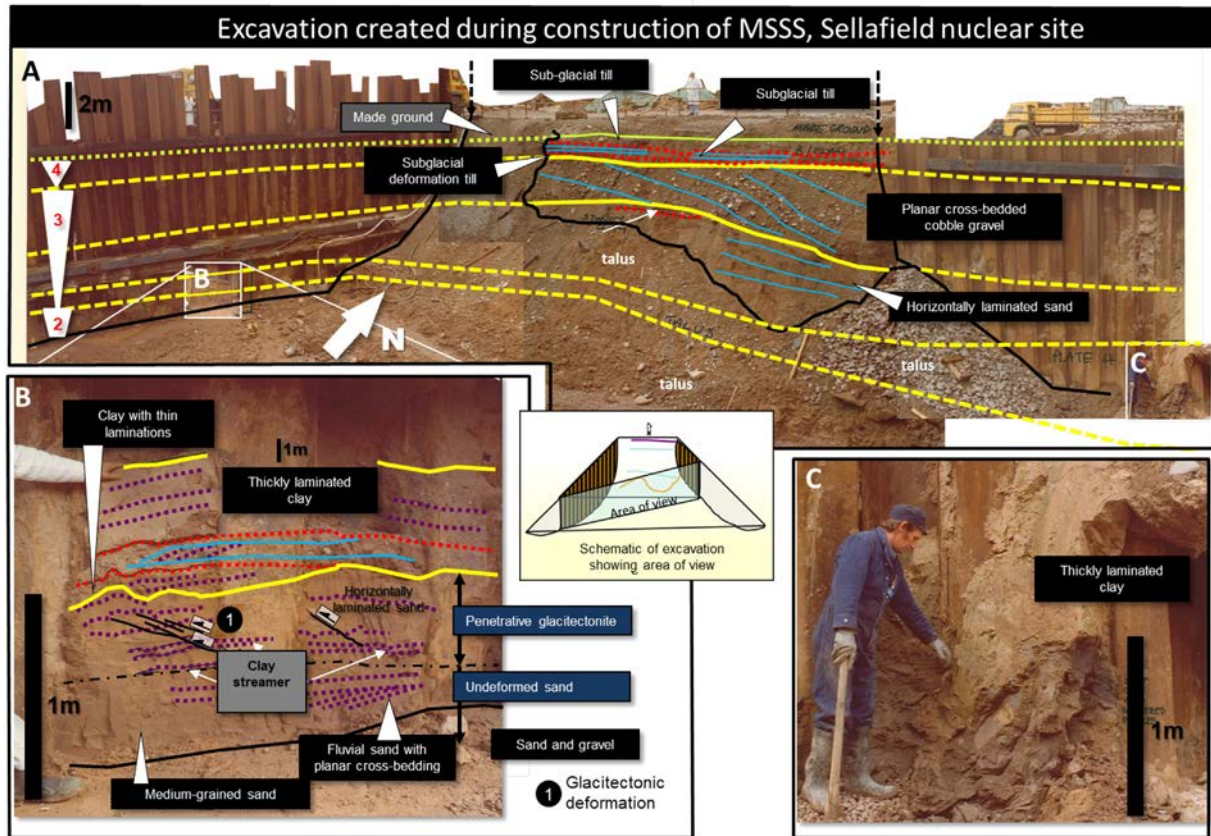


Fig. 11. Units of glacial material exposed in excavation during the construction of MSSS: (A) whole exposure – note view is panoramic – see Fig. 1(C) for locations; (B) detail of deformation clay and penetrative glaciectonite in underlying sand (C) detail of thick clay – laminations are likely to be a fabric rather than depositional laminations (NB: please see yellow rectangle on Fig. 8 for approximate location with respect to sequence penetrated by BH7).

compared to outwash deposits in Sequence 1), suggesting a retrograding or retreating outwash fan system. Sequence 4 comprises three sub-units of subglacial deformation till sensu Larsen and Piotrowski (2003). The remainder of Sequence 4 is missing, presumed eroded or not deposited.

This exercise is useful because (a) it presents a repeating set of cyclic sequences that are likely to be present certainly in the immediate vicinity of BH7 within the site, thus allowing the geological 3D modeller a framework of possible units and unit boundaries to look for within geotechnical logs, and to base correlation upon, and (b) it provides a suggestion of the probable depositional evolution of the location, that can be taken much further. These are discussed in Section 8.

8. Discussion

8.1. Use of MSCL and XCT data for assessment and modelling of potentially contaminated land in poorly exposed industrial locations

The previous section illustrates how MSCL and XCT data can provide the basis for more accurate and geologically valid lithological description of borehole core, including a far more reliable identification of boundaries between lithological units, and thus, even on their own, a geologically valid basis for correlation from borehole to borehole (assuming a similar approach has been undertaken for other boreholes) can be made. Units are now bounded by erosion surfaces identified using geophysical evidence, rather than by estimating where a surface may lie between the locations of samples extracted from the borehole. Correlation is made easier by the definition of four cyclic glacial

advance/retreat sequences, the application of which to the other boreholes in the study is considered reasonable considering their closeness (Fig. 1). Nearly all the unit boundaries have been modified (moved) and since some lithological units have been redefined new unit bounding surfaces (unit boundaries) have been created. Fig. 10 (A) illustrates the borehole correlation panel created by correlation of units defined according to bulk lithology, utilising descriptions which are themselves based on BS5930/Eurocode 7 (British Standards Institution, 2015) (British Standards Institution, 2005). Borehole 7 is also shown in Fig. 10(B) to illustrate the redefinition of lithological units and unit bounding surfaces that interpretation of lithological units and unit bounding surfaces that interpretation of MSCL and XCT data has allowed (as shown in Fig. 10(C)). The application of the new borehole log to the correlation panel is shown in Fig. 10(D). Original interpretation lines are shown as black dashes, with new interpretations shown in continuous black lines (dashed purple lines represent the base/top of each of the cyclical sequences 1 to 4).

Whilst this is one of perhaps several interpretations, it is immediately clear that (a) the four cycles can be applied to the sequence represented by the correlation panel, but that (b) the interpreted boundaries for the other boreholes in the panel may be suspect, which is something that examination of MSCL/XCT data could significantly address.

8.2. Application of MSCL/XCT interpretation to study of regional geological history

In the late 1970s a photographic record was made of the geology exposed by an excavation dug during construction of foundations for the MSSS. Although somewhat hindered by the resolution, it is possible to

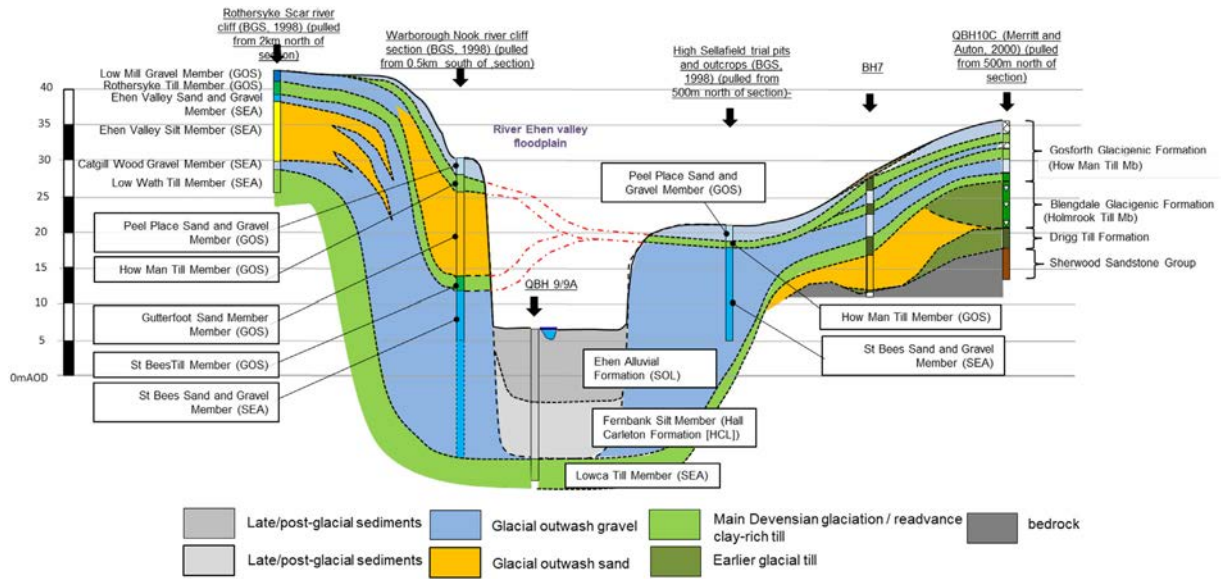


Fig. 12. Revision to geological section along Line A (shown in Fig. 2), incorporating new interpretation from BH7.

identify similar units and even correlate them to those shown in Fig. 8: An upper sub-glacial till is likely to correspond to the uppermost subglacial deformation till identified on the graphic log (forming the lowest and only unit present in glacial advance/retreat Sequence 4 (see Fig. 11A). Underlying gravel and sand units correspond to glacial outwash deposits overlying another subglacial till and forming cyclic Sequence 3, whilst the deformed and undeformed sand underlying this unit forms the top of cyclic Sequence 2 (see also Fig. 8).

These interpretations can also be used to update or confirm interpretations of regional geological history is illustrated in Fig. 12. Here the new BH7 log is slotted into the schematic Line A section shown previously in Fig. 2. The interpretation has required little in the way of modification, with the new log appearing in fact, to confirm it. However, there is much unused information within the MSCL and XCT data that could be applied, for example, to a much more extensive treatment of sedimentary architecture than can be provided within the scope of this paper.

9. Conclusions

Borehole core obtained from a borehole drilled through Quaternary-aged, unconsolidated, glacially-derived sediments within the Separation Area of Sellafield nuclear site (one of the boreholes drilled for the project described by Kuras, et al., (2016), was analysed on-site using Geotek’s mobile multi-sensor core logging (MSCL) and X-ray computed tomography (XCT) laboratory. Geophysical logs comprising natural gamma, resistivity, magnetic susceptibility, density and fracture porosity, along with XCT images of the core, obtained in three orientations, were examined and compared to lithological log descriptions to develop an understanding of the geophysical characteristics of the succession and to provide revised log descriptions to a higher resolution than possible under national and international geotechnical standards. Utilising the geophysical logs, lithological unit bounding surfaces were identified with much improved accuracy, and combined with revised log descriptions to produce a detailed graphic sedimentary log.

A comparison of this with (i) geotechnical logs of the other boreholes created as part of the 2016 study (Kuras et al., 2016) and (ii) regional boreholes and outcrops already described using the lithostratigraphic outline of (Merritt and Auton, 2000) provides the following conclusions:

- (a) Core analysis using MSCL and XCT could vastly improve borehole correlation and thus reduce uncertainty 3D geological subsurface models for complex industrial sites where geological exposure is poor.
- (b) The improved interpretation can be used to tie to regional interpretations which (in the case of Sellafield nuclear site) has proved difficult, if not impossible.

Declaration of Competing Interest

The authors declare that they have no known competing financial interests or personal relationships that could have appeared to influence the work reported in this paper.

Acknowledgements

This paper is published with the permission of Sellafield Ltd. (on behalf of the Nuclear Decommissioning Authority), Geotek Ltd, and the National Nuclear Laboratory, UK. BGS authors publish with permission of the Executive Director of the British Geological Survey (UKRI). The authors thank Sellafield Ltd for provision of borehole data, and for permission to reproduce the photograph used in Fig 11. Smith was funded by a Royal Society Industry Fellowship and the National Nuclear Laboratory (NNL) Core Science Group Research and Development (R&D) programme. Nick Atherton and Josephine Wren (Sellafield Ltd) and Adrian Bull (NNL) are thanked for assistance.

References

Nirex, 1997. *The Quaternary of the Sellafield area S/97/002*, s.l.: Nirex.
 Adams, J.A.S., Gaspririni, P., 1970. *Gamma-Ray Spectrometry of Rocks*. Elsevier, Amsterdam, New York, London.
 Akhurst, M.C., et al., 1997. *Geology of the West Cumbria District. Memoir of the British Geological Survey, Sheets 28, 37 and 47 (England and Wales)*. British Geological Survey, Nottingham.
 Barnes, R.P., Ambrose, K., Holliday, D.W., Jones, N.S., 1994. *Lithostratigraphic subdivision of the Triassic Sherwood Sandstone Group in west Cumbria*. Proc. Yorks. Geol. Soc. 50, 51–60.
 Becker, M., Jardine, M.A., Miller, J.A., Harris, M., 2016. *X-Ray Computed Tomography - a Geometallurgical Tool for 3D Textural Analysis of Drill Core?*. Perth, WA, The Third AUSIMM International Geometallurgy Conference.
 Benn, D.I., 1995. *Fabric signature of subglacial till deformation, Bredamerkurjokull, Iceland*. Sedimentology 42, 735–747.

- Benn, D.I., Evans, D.J.A., 1998. *Glaciers and Glaciations*. Arnold, London.
- Boulton, G.S., Hindmarsh, R.C.A., 1987. Sediment deformation beneath glaciers: Rheology and geological consequences. *J. Geophys. Res.* 92, 9059–9082.
- Boulton, G.S., Jones, A.S., 1979. Stability of temperate ice caps and ice sheets resting on beds of deformable sediments. *J. Glaciol.* 24, 229–243.
- Boyce, R.E., 1973. Appendix 1. Physical property methods. In: Edgar, N.T., Saunders, J.B. (Eds.), *Initial Reports Deep Sea Drilling Project 15*. US Government Printing Office, Washington DC, pp. 1115–1128.
- Brannon, H.H.J., Osaba, J.S., 1956. Spectral gamma-ray logging. *J. Pet. Technol.* 8, 30–35.
- Browne, M., et al., 2000. *Field Guide: The Quaternary Geology of West Cumbria*. s.l. The Geological Society of London Environment Group.
- Busby, J.P., Merritt, J.W., 1999. Quaternary deformation mapping with ground penetrating radar. *J. Appl. Geophys.* 41, 75–91.
- Cnudde, V., Boone, M.N., 2013. High-resolution X-ray computed tomography in geosciences: a review of the current technology and applications. *Earth Sci. Rev.* 123, 1–17.
- Cripps, A.C., McCann, D.M., 2000. The use of the natural gamma log in engineering geological investigations. *Eng. Geol.* 55, 313–324.
- Cross, M., Attya, A., Evans, D.J.A., 2018. The susceptibility of glacial deposits to liquefaction under seismic loading conditions: a case study relating to nuclear characterization in West Cumbria. *Proc. Yorks. Geol. Soc.* 62, 116–132.
- Denis, M., Guiraud, M., Konate, M., Buoncristiani, J.F., 2010. Subglacial deformation and water-pressure cycles as a key for understanding ice stream dynamics: evidence from the late Ordovician succession of the Djado Basin (Niger). *International Journal of Earth Science (Geol Rundsch)* 99, 1399–1425.
- Dickson, B.H., Bailey, R.C., Gratsy, J.A., 1981. Utilizing multi-channel airborne gamma-ray spectra. *Can. J. Earth Sci.* 18, 1793–1801.
- Durance, P., Jowitz, S.M., Bush, K., 2014. An assessment of portable X-ray fluorescence spectroscopy in mineral exploration. *Kurnalpi Terrane, Eastern Goldfields Superterrane, Western Australia. Applied Earth Sciences (Trans. Inst. Min. Metall. B)* 123, 150–163.
- Eastwood, T., Dixon, E.E.L., Hollingworth, S.E., Smith, B., 1931. *The geology of the Whitehaven and Workington District. Memoir of the Geological Survey of Great Britain, England and Wales, Sheet 23*. s.l.:Geological Survey of Great Britain, England and Wales.
- Evans, H. B., 1970. Gamma-ray attenuation density scanner. In: M. N. A. Peterson & et al, *Initial Reports Deep Sea Drilling Project 2*. Washington DC: US Government Printing Office, pp. 460–471.
- Faul, H., 1954. *Nuclear Geology*. s.l. John Wiley and Sons.
- Fellgett, M.w., et al., 2019. Lithological constraints on borehole wall failure: a study on the pennine coal measures of the United Kingdom. *Front. Earth Sci.* 7 (163).
- Fisher, L., et al., 2014. Resolution of geochemical and lithostratigraphic complexity: a work flow for application of portable X-Ray fluorescence to mineral exploration. *Geochem. Explor. Environ. Anal* 14, 149–159.
- Flanagan, W.D., et al., 1991. *A new generation nuclear logging system*. s.l. Soc. Prof. Well Log Analysts Ann. Log. Symp, 33nd Trans Y1–Y25.
- Fresia, B., Ross, P.-S., Gloaguen, E., Bourke, A., 2017. Geological discrimination based on statistical analysis of multi-sensor core logging data in the Matagami VMS district, Quebec, Canada. *Ore Geology Reviews* 80, 552–563.
- Gazley, M.F., Fisher, L.A., 2014. A Review of the Reliability and Validity of Portable X-Ray Fluorescence Spectrometry (pXRF) Data. *Mineral Resource and Ore Reserve Estimation - the AusIMM Guide to Good Practice*, second ed. The Australian Institute of Mining and Metallurgy, Melbourne.
- Gazley, M.F., et al., 2014. Objective geological logging using portable XRF geochemical multi-element data at Plutonic Gold Mine, Marymia Inlier, Western Australia. *Journal of Geochemical Exploration* 143, 74–83.
- Goldberg, D., 1997. The role of downhole measurements in geology and geophysics. *Rev. Geophys.* 35 (3), 315–342.
- Gratsy, R.L., Glynn, J.E., Grant, J.A., 1985. The analysis of multichannel airborne gamma-ray spectra. *Geophysics* 50, 2611–2620.
- Gunn, P.J., 1978. Inversion of airborne radiometric data. *Geophysics* 43, 133–142.
- Gunn, D.E., Best, A.I., 1998. A new automated nondestructive system for high resolution multi-sensor core logging of open sediment cores. *Geo-Mar. Lett.* 18, 70–77.
- Gupta, L.P., et al., 2019. Examination of gas hydrate-bearing deep ocean sediments by X-ray Computed Tomography and verification of physical measurements of sediment. *Mar. Pet. Geol.* 108, 239–248.
- Haubitz, B., et al., 1988. Computed tomography of Archeopterix. *Palaeobiology* 14, 206–213.
- Herrmann, W., et al., 2001. Short wavelength infrared (SWIR) spectral analysis of hydrothermal alteration zones associated with base metal sulfide deposits at Rosebery and Western Tharsis, Tasmania and Highway-Reward, Queensland. *Economic Geology* 96, 939–955.
- Hickock, S.R., Dreimanis, A., 1992. Deformation till in the Great Lake region, implications for rapid flow along the south-central margin of the Laurentide Ice Sheet. *Canadian Journal of Earth Sciences* 29, 1565–1579.
- Hill, L.J., Sparks, R.S., Roughier, J.C., 2012. Risk assessment and uncertainty in natural hazards. In: Roughier, J., Sparks, S., Hill, L. (Eds.), *Risk and Uncertainty Assessment for Natural Hazards*. s.l. Cambridge University Press, pp. 1–18.
- Hounsfield, G. N., 1972. *A method of and apparatus for examination of a body by radiation such as X-or gamma-radiation*. UK, Patent No. British Patent No 1,283,915.
- Hounsfield, G.N., 1973. Computerized transverse axial scanning (tomography): part 1. Description of system. *British Journal of Radiology* 46, 1016–1022.
- Huddart, D., 1970. Aspects of Glacial Sedimentation in the Cumberland Lowland. University of Reading, Reading.
- Huddart, D., 1971a. A relative glacial chronology from the tills of the Cumbrian lowland. *Proceedings of the Cumberland Geological Society* 3, 21–32.
- Huddart, D., 1971b. Textural distinction between Main Glaciation and Scottish Readvance tills in the Cumberland Lowland. *Geol. Mag.* 108, 317–324.
- Huddart, D., 1977. Gutterby Spa - Annaside Banks Moraine and St Bees Moraine. In: Tooley, M.J. (Ed.), *The Isle of Man, Lancashire coast and Lake District. Field guide for excursion A4 X INQUA Congress, Geo Abstracts*. Norwich: s.n, pp. 38–40.
- Huddart, D., 1991. The glacial history and glacial deposits of the North and West Cumbrian lowlands. In: Ehlers, J., Gibbard, P.L., Rose, J. (Eds.), *Glacial Deposits in Great Britain and Ireland*. Balkema, Rotterdam, pp. 151–167.
- Huddart, D., 1994. The late Quaternary glacial sequence: Landforms and environments in coastal Cumbria. In: Boardman, J., Walden, J. (Eds.), *The Quaternary of Cumbria: Field Guide*. The Quaternary Research Association, Oxford, pp. 59–77.
- Huddart, D., Clarke, R., 1994. Conflicting interpretations of glacial sediments and landforms in Cumbria. *Proceedings of the Cumberland Geological Society* 5, 419–436.
- Huddart, D., Tooley, M.J., 1972. *Field Guide to the Cumberland Lowland*. Quaternary Research Association, Cambridge.
- British Standards Institution, 2005. Eurocode 7: Geotechnical Design Part 2: Ground Investigation and Testing. British Standards Institution London prEN, London (1997–2).
- British Standards Institution, 2015. BS 5930: 2015 - the Code of Practice for Site Investigations. British Standards Institution, Milton Keynes.
- Jardine, M.A., Miller, J.A., Becker, M., 2018. Coupled X-ray computed tomography and grey level co-occurrence matrices as a method for quantification of mineralogy and texture in 3D. *Comput. Geosci.* 111, 105–117.
- Joly, J.J., 1909. *Radioactivity and Geology*. Archibald Constable, London.
- Jones, N.S., Ambrose, K., 1994. Triassic sandy braidplain and aeolian sedimentation in the Sherwood Sandstone Group of the Sellafeld area, west Cumbria. *Proceedings of the Yorkshire Geological Society* 50, 61–76.
- Kessler, H., Mathers, S., Sobisch, H.-G., 2009. The capture and dissemination of integrated 3D geospatial knowledge at the British Geological Survey using GIS3D software and methodology. *Comput. Geosci.* 35 (6), 1311–1321.
- Ketcham, R.A., Carlson, W.D., 2001. Acquisition, optimization and interpretation of X-ray computed tomographic imagery: applications to the geosciences. *Comput. Geosci.* 27 (4), 381–400.
- Killeen, P.G., 1982. Gamma-ray logging and interpretation. In: Fitch, A.A. (Ed.), *Developments in Geophysical Exploration Methods*. 3. Applied Science Publishers, pp. 95–150.
- Kuras, O., et al., 2016. Geoelectrical monitoring of simulated subsurface leakage to support high-hazard nuclear decommissioning at the Sellafeld Site, UK. *Science of the Total Environment* 566–567, 350–359.
- Larsen, N.K., Piotrowski, J.A., 2003. Fabric pattern in a basal till succession and its significance for reconstructing subglacial processes. *J. Sediment. Res.* 73 (5), 725–734.
- Le Vaillant, M., et al., 2014. Use and calibration of portable X-ray fluorescence analysers: application to lithochemical exploration for komatiite-hosted nickel sulphide deposits. *Geochem. Explor. Environ. Anal.* 14, 199–209.
- Lemon, A.M., Jones, N.L., 2003. Building solid models from boreholes and user-defined cross-sections. *Comput. Geosci.* 29, 547–555.
- Letzer, J.M., 1981. The Upper Eden Valley (Ravenstonedale). In: Boardman, J. (Ed.), *Eastern Cumbria Field Guide*. S.l. Quaternary Research Association, pp. 43–60.
- Lovberg, L., Wollenberg, H., Rose-Hansen, J., Nielsen, B.L., 1972. Drill-core scanning for radioelements by gamma-ray spectrometry. *Geophysics* 37, 675–693.
- van der Meer, J.J.M., 1993. Microscopic evidence of subglacial deformation. *Quat. Sci. Rev.* 12, 553–587.
- van der Meer, J.J.M., 1997. Particle and aggregate mobility in till: microscopic evidence of subglacial processes. *Quat. Sci. Rev.* 12, 827–831.
- Mees, F., Swennen, R., Van Geet, M., Jacobs, P., 2003. Applications of X-ray Computed Tomography in the Geosciences. Special Publication of the Geological Society 215, 1–6.
- Merritt, J.W., Auton, C.A., 2000. An outline of the lithostratigraphy and depositional history of Quaternary deposits in the Sellafeld district, west Cumbria. *proceedings of the Yorkshire Geological Society* 53 (2), 129–154.
- Miall, A.D., 2006. Reconstructing the architecture and sequence stratigraphy of the preserved fluvial record as a tool for reservoir development: a reality check. *AAPG Bull.* 90, 989–1002.
- Petrovic, A.M., Siebert, J.E., Rieke, P.E., 1982. Soil bulk density analysis in three dimensions by computed tomographic scanning. *Soil Sci. Soc. Am. J.* 46, 445–450.
- Phillips, E.R., Auton, C.A., 2000. Micromorphological evidence for polyphase deformation of glaciolacustrine sediments from Strathspey, Scotland. In: Maltman, A.J., Hubbard, B., Hambrey, M.J. (Eds.), *Deformation of Glacial Material*. The Geological Society of London, Special Publication, London, pp. 279–291.
- Phillips, E.R., Merritt, J.W., Auton, C.A., Colledge, N.R., 2007. Microstructures developed in subglacially and proglacially deformed sediments: faults, folds and fabrics, and the influence of water on the style of deformation. *Quaternary Science Reviews* 26, 720–738.
- Phillips, E., van der Meer, J.J.M., Ferguson, A., 2011. A new 'microstructural mapping' methodology for the identification, analysis and interpretation of polyphase deformation within subglacial sediments. *Quaternary Science Reviews* 30, 2570–2596.
- Preiss, K., 1968. Non-destructive laboratory measurement of marine sediment density in a core barrel using gamma radiation. *Deep-Sea Res.* 15, 401–407.
- Räsänen, M.E., et al., 2009. A shift from lithostratigraphic to allostratigraphic classification of Quaternary glacial deposits. *GSA Today* 19 (2).
- Rawson, P.F., et al., 2002. *Stratigraphical Procedure: Geological Society Professional Handbook*. The Geological Society, London.
- Robinson, S.G., 1993. Lithostratigraphic applications for magnetic susceptibility logging of deep-sea sediment cores: Examples from ODP Leg 115. In: Hailwood, E.A., Kidd, R.B. (Eds.), *High Resolution Stratigraphy*. Geological Society of London, London, pp. 65–98.

- Schultheis, P.J., McPhail, S.D., 1989. An automated P-wave logger for recording fine-scale compressional wave velocity structures in sediments. *Proc. ODP Sci. Results* 108, 407–413.
- Schultheis, P.J., Weaver, P.P.E., 1992. Multi-sensor core logging for science and industry. *Proceedings Oceans 92, Mastering the Oceans Through Technology 2*, 608–613.
- Smirnov, A., Boisvert, E., Paradis, S.J., 2008. Support vector machine for 3D modelling from sparse geological information of various origins. *Comput. Geosci.* 34 (2), 127–143.
- Smith, B., 1932. The glacier-lakes of Esdale, Miterdale and Wasdale, Cumberland; and the retreat of the ice during the main glaciation. *Quarterly Journal of the Geological Society, London* 88, 57–83.
- Smith, N., 2009. *Record of exploratory trial pits excavated in the floor of Vault 9 excavation, LLWR, NNL10174*, s.l. Low Level Waste Repository Ltd.
- Smith, N., Cooper, S., 2004. *SCLS Phase 1 - Sellafield Geological Conceptual Model*. NSTS 4866 (03/ENO 130/7/8) Issue. 1 ed. British Nuclear Fuels plc.
- Smith, N.T., Merritt, J.W., 2008. Further insights into the Quaternary superficial geology of West Cumbria, using 3D geological modelling: implications for Devensian palaeogeographic evolution. 33rd International Geoscience Convention, Oslo, Norway.
- Smith, B., et al., 2008. 3D Modelling of Geology and Soils: A Case Study from the UK. In: Hartemink, A.E., McBratney, A., Mendonça-Santos, M. (Eds.), *Digital Soil Mapping with Liited Data*. Springer, Dordrecht.
- Thomas, G.S.P., Chiverrell, R.C., 2007. Structural and depositional evidence for repeated ice-marginal oscillation along the eastern margin of the late Devensian Irish Sea Ice Stream. *Quat. Sci. Rev.* 26, 2375–2405.
- Thomas, G.S.P., Connaughton, M., Dackome, R.V., 1985. Facies variation in a supraglacial outwash Sandur from the Isle of Man. *Geol. J.* 20, 193–213.
- Tremblay, T., Nastev, M., Lamothe, M., 2010. Grid-based hydrostratigraphic modelling of the Quaternary sequence in the Chateauguay River Watershed, Quebec. *Water Resources Journal* 35 (4), 377–398.
- Trotter, F.M., 1922. Report from the Cumberland District. In: *Summary of Progress of the Geological Survey of Great Britain for 1921*. s.l.:Geological Survey of Great Britain. pp. 46–48.
- Trotter, F.M., 1923. Report from the Cumberland District. In: *Summary of Progress of the Geological Survey of Great Britain for 1922*. s.l.:Geological Survey of Great Britain. pp. 61–63.
- Trotter, F.M., 1929. The glaciation of Easten Edenside, the Alston Block and the Carlisle Plain. *Quarterly Journal of the Geological Society, London* 85, 549–612.
- Trotter, F.M., Hollingworth, S.E., 1932. The glacial sequence in the North of England. *Geol. Mag.* 69, 374–380.
- Trotter, F.M., Hollingworth, S.E., Eastwood, T., Rose, W.C., 1937. *Gosforth District. Memoir of the Geological Survey of Great Britain, England and Wales. Sheet 37*. s.l.:Geological Survey of Great Britain, England and Wales.
- Turner, A.K., 2006. Challenges and trends for geological modelling and visualization. *Bull. Eng. Geol. Environ.* 65 (2), 109–127.
- Vasiliev, A., et al., 2011. A new natural gamma radiation measurement system for marine sediment and rock analysis. *J. Appl. Geophys.* 75 (3), 455–463.
- Velasco, V., et al., 2013. The use of GIS-based 3D geological tools to improve hydrogeological models of sedimentary media in an urban environment. *Environ. Earth Sci.* 68, 2145–2162.
- van der Wateren, F.M., 1995. Process of glaciotectionism. In: Menzies, J. (Ed.), *Glacial Environments, Vol 1: Modern Glacial Environments*. Butterworth-Heinemann, Oxford, pp. 309–335.
- van der Wateren, F.M., Kluiving, S.J., Bartek, L.R., 2000. In: Maltman, A.J., Hubbard, B., Hambrey, M.J. (Eds.), *Kinematic indicators of subglacial shearing*. Geological Society of London, Special Publication, Deformation of Glacial Material. London, pp. 259–278.
- Wellmann, J.F., Horowitz, F.G., Schill, E., Regenauer-Lieb, K., 2010. Towards incorporating uncertainty of structural data in 3D geological inversion. *Tectonophysics* 490 (3–4), 141–151.
- Yang, K., Huntington, J.F., Gemmel, J.B., Scott, K.M., 2011. Variations in composition and abundance of white mica in the hydrothermal alteration system at Hellyer, Tasmania, as revealed by infrared reflectance spectroscopy. *Journal of Geochemical Exploration* 108, 143–156.
- Zhu, L., et al., 2012. Building 3D solid models of sedimentary stratigraphic systems from borehole data: an automatic method and case studies. *Engineering Geology* 127, 1–13.